

## Multi-DBD plasma actuator for flow separation control around NACA 0012 and NACA 0015 airfoil models

**Abstract.** In this paper application of innovative multi-DBD plasma actuator for flow separation control is presented. The influence of the airflow generated by this actuator on the flow around NACA 0012 and NACA 0015 airfoil models was investigated. The results obtained from 2D PIV measurements showed that the multi-DBD actuator with floating interelectrode can be attractive for leading and trailing edge separation control.

**Streszczenie.** W niniejszej pracy zaprezentowano innowacyjny aktuator plazmowy z elektrodą o potencjale pływającym. Aktuator ten zastosowano do aktywnej kontroli przepływu wokół elementów aerodynamicznych. Rezultaty badań wskazują, że badany aktuator umożliwia kontrolę oderwania warstwy przyściennej wokół modeli skrzydła NACA 0012 i NACA 0015. (Aktuator plazmowy multi-DBD do kontroli oderwania warstwy przyściennej wokół modeli skrzydła NACA 0012 i NACA 0015)

**Keywords:** plasma, airflow control, surface dielectric barrier discharge, DBD.

**Słowa kluczowe:** plazma, kontrola przepływu, powierzchniowe wyładowanie barierowe, DBD.

### Introduction

Nowadays, the importance of an air transport in the world economy is constantly growing. Unfortunately, the heavy air traffic is the source of pollutions which are harmful for a human health and an environment. Thus, the great research effort is directed to make aircrafts more human and environment friendly. This objective can be achieved e.g. by improving aircraft aerodynamics. Unfortunately, using the conventional technologies, further improvements of the aircraft aerodynamics is severely limited. Thus, the new solutions like usage of dielectric barrier discharge (DBD) plasma actuators for active airflow control around aerodynamic elements are under development.

The DBD actuators are devices using plasma generated by the surface dielectric barrier discharge for active airflow control [1-3]. The surface DBD occurs when a voltage is applied to electrodes which are set on the top and bottom sides of a dielectric material. The plasma generated by the DBD actuator induces electrohydrodynamic (EHD) flow which allows to modify airflow around aerodynamic elements. Using DBD actuators it is possible to control the boundary layer flow separation or laminar-turbulent flow transition.

When the critical angle of attack of the airfoil is exceeded (so called stall) the boundary layer flow separation occurs. When the stall takes place the lift of the airfoil is drastically reduced and the drag is increased. In case of aircrafts stall leads to an autorotation and a sudden reduction of an altitude. Therefore, prevention of the stall using DBD actuators could have significant meaning for improvement of the aircraft operation and safety.

Currently, researches on DBD plasma actuators for flow control are popular and are performed in many laboratories all over the world [4-8]. Although, the published experimental results showed that DBD plasma actuators are capable of modifying airflow around aerodynamic elements they are still not used for practical applications. The main reason of this is relatively low airflow velocity generated by the DBD actuator (for single-DBD actuator generated airflow do not exceed 5-6 m/s) which is not adequate for efficient control of the flow around aircraft wing. Thus, more investigations that will allow us the better understanding properties of the surface dielectric barrier discharge and mechanism of inducing EHD flow are needed.

In this paper the ability of an innovative multi-DBD actuator with floating interelectrode to improve the

aerodynamic performance of the NACA 0012 and NACA 0015 airfoils models is presented. Our studies of the flow separation control around these airfoils were based on the velocity fields measured by 2D Particle Image Velocimetry (PIV) technique. Performed investigations showed that our multi-DBD actuator with floating interelectrode can be attractive for aerodynamic applications.

### Experimental set-up

#### Multi-DBD actuator with floating interelectrode

The multi-DBD actuator with floating interelectrode used for investigations of a leading and a trailing edge flow separation control around airfoil models is presented in Figure 1.

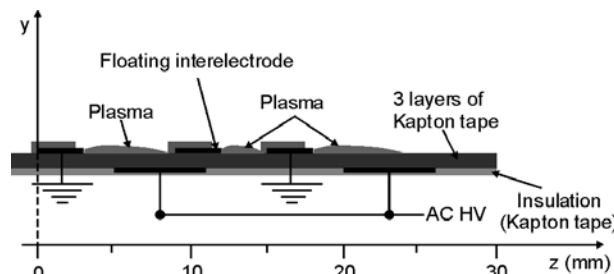


Fig.1. Schematic side view of the multi-DBD actuator with floating interelectrode used for a flow separation control

To fit the multi-DBD actuator to an airfoil model a flexible material (3 layers of a 45  $\mu\text{m}$ -thick Kapton tape) was used as a main dielectric barrier. All electrodes used in this actuator were made of a 50  $\mu\text{m}$ -thick copper tape. The length of electrodes was 500 mm. The floating and grounded electrodes were on the flow active side of the dielectric material and were partially insulated with Kapton tape (as it is shown in Figure 1). The HV electrodes were on the opposite side of the dielectric barrier and were fully insulated. The smooth HV electrodes were 6 mm wide (Fig. 2a), while the saw-like grounded electrodes and the floating interelectrode were 3 mm wide (Figs. 2b and 2c). The floating interelectrode consisted of a series of separated saw teeth. The saw-like electrodes were used because our previous results showed that with such a electrodes the DBD starts at lower voltage, produces more homogenous plasma and the higher airflow velocities compared with the DBD with smooth electrodes [9].

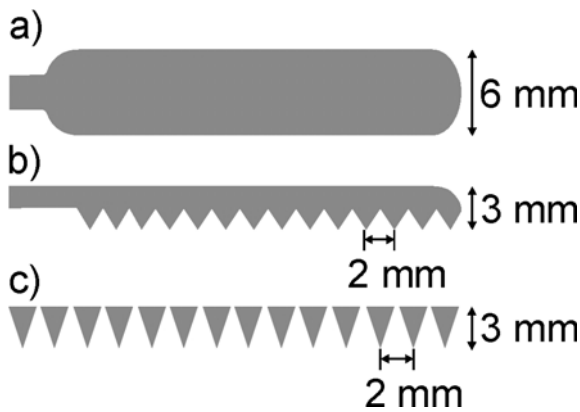


Fig.2. Schematic top view of the smooth HV electrode (a), the saw-like grounded electrode (b) and separated saw teeth of the floating interelectrode (c)

#### Airfoil models

Two airfoil models with fixed multi-DBD actuator were prepared. In both cases investigated airfoil model was 200 mm wide in chord and 595 mm wide in spanwise direction. The length of the actuator was 500 mm (spanwise).

The first airfoil model NACA 0012 (Fig. 3) was used for the leading edge flow separation control investigations. The first DBD generated by the multi-DBD actuator started at position  $z/C = 4\%$  ( $z$  - distance from the leading edge,  $C$  - chord length).

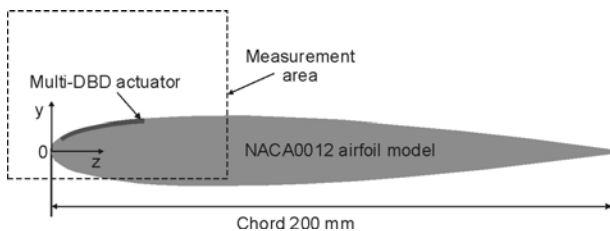


Fig.3. Schematic side view of the NACA 0012 airfoil model. The measurement area is marked with a broken line

The second airfoil model NACA 0015 (Fig. 4) was used for trailing edge flow separation control experiments. In this case the first DBD generated by the multi-DBD actuator started at position  $z/C = 52\%$ .

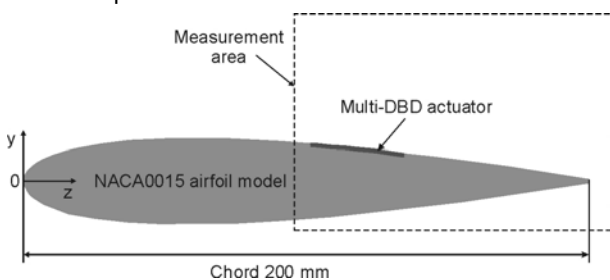


Fig.4. Schematic side view of the NACA 0015 airfoil model. The measurement area is marked with a broken line

The photo of the investigated NACA 0012 airfoil model with integrated multi-DBD actuator is presented in Figure 5.

#### Experimental apparatus

The experimental set-up for flow separation control investigations is presented in Figure 6. It consisted of an AC power supply, a 2D PIV equipment for measurements of the flow velocity fields and a wind tunnel where the airfoil models were placed.

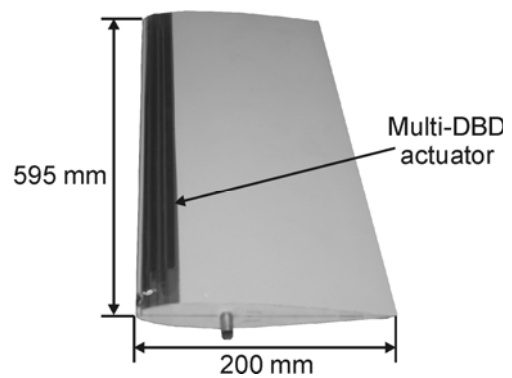


Fig.5. Image of the NACA 0012 airfoil model with integrated multi-DBD actuator

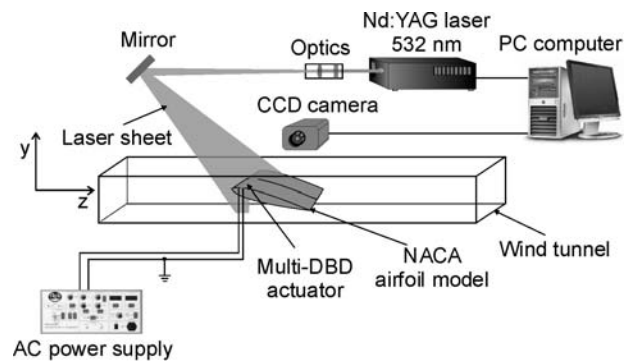


Fig.6. Experimental set-up for flow separation control measurements

The sinusoidal high voltage (frequency 1.5 kHz) applied to the multi-DBD actuator was generated by a HV function generator (Trek, model PM04015A). During the flow separation control investigations applied peak-to-peak high voltage was 13 kV or 15 kV.

The experiments were carried out in an ambient air at atmospheric pressure. A test section of the wind tunnel was 600 mm wide and 480 mm high. A free stream velocity in the wind tunnel during measurements was 10 m/s, 15 m/s or 20 m/s and the turbulence level was below 0.1%.

The 2D PIV system for measuring the flow velocity field was composed of a double Nd:YAG laser system ( $\lambda = 532$  nm), a cylindrical telescope, a CCD camera and a PC computer. A cigarette smoke was used as a seed. The images of the seed particles (called a flow images) following the airflow around NACA 0012 or NACA 0015 airfoil models were recorded by FlowSense M2 camera. The CCD camera sensor size was 1600 pixels  $\times$  1186 pixels.

150 pairs of the PIV instantaneous flow images of the airflow around NACA airfoil models were captured and transmitted to the PC computer for a digital analysis. For the digital analysis Dantec Flow Manager software was used. An adaptive cross-correlation algorithm was applied to the set of 150 image pairs to compute 150 instantaneous flow velocity fields. The interrogation window during the cross-correlation procedure was 32 pixels  $\times$  16 pixels. The overlap between neighbouring interrogation windows was 25%. Basing on these instantaneous flow velocity fields the time-averaged airflow velocity fields were calculated.

#### Results

The leading edge (with NACA 0012 airfoil model) and trailing edge (with NACA 0015 airfoil model) flow separation control experiments were performed for three values of the

free stream velocity (10 m/s, 15 m/s or 20 m/s) and for angles of attack between 8 and 15 degree.

In the case of leading edge flow separation investigations the observation area (marked with a broken line in Figure 3) was 77 mm × 57 mm and the spatial resolution of obtained vector velocity fields was 1.2 mm × 0.6 mm. The examples of obtained time-averaged contour velocity maps for leading edge flow separation control investigations with the multi-DBD actuator turned off and turned on are presented in Figures 7 and 8, respectively. In this case the free stream velocity was  $V_0 = 15 \text{ m/s}$  ( $Re = 2 \times 10^5$ ) and an angle of attack was  $11^\circ$ . The high voltage applied to multi-DBD actuator was  $15 \text{ kV}_{pp}$ . As it can be seen, when the multi-DBD actuator was off the airflow was separated near the leading edge of the airfoil and a large vortex existed. Thus, the airfoil was in the stall regime. However, an activation of the multi-DBD actuator caused the airflow reattachment.

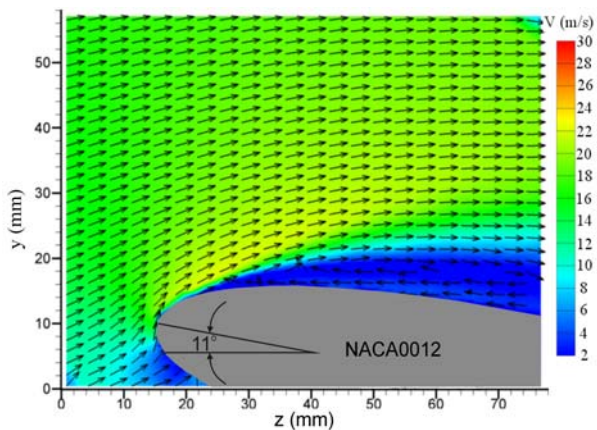


Fig.7. Time-averaged contour velocity map of the airflow around the NACA 0012 airfoil model. Free stream velocity  $V_0 = 15 \text{ m/s}$ ; angle of attack  $11^\circ$ . Plasma OFF – separated airflow

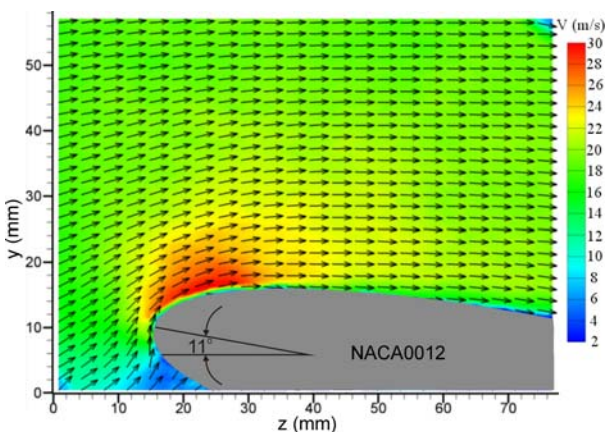


Fig.8. Time-averaged contour velocity map of the airflow around NACA 0012 airfoil model. Free stream velocity  $V_0 = 15 \text{ m/s}$ ; angle of attack  $11^\circ$ . Plasma ON – airflow reattached. The applied sine-wave voltage was  $15 \text{ kV}_{pp}$  and the frequency was 1.5 kHz

Similar effect of an actuation was observed for trailing edge flow separation experiments. In this case the observation area (marked with a broken line in Figure 4) was  $112 \text{ mm} \times 83 \text{ mm}$  and the spatial resolution of obtained vector velocity fields was  $1.7 \text{ mm} \times 0.8 \text{ mm}$ . In Figure 9 the example of obtained time-averaged contour velocity map of the airflow around NACA 0015 airfoil model (without an actuation) is presented. In this case the free stream velocity was  $V_0 = 10 \text{ m/s}$  ( $Re = 1.3 \times 10^5$ ) and the angle of attack was  $14^\circ$ . As it can be seen, the flow above the airfoil

model was separated (stall regime) and large vortex existed near the trailing edge of the airfoil model. When the multi-DBD actuator was activated almost fully reattachment of the airflow occurred and only small vortex close the trailing edge of the airfoil can be observed (Fig. 10).

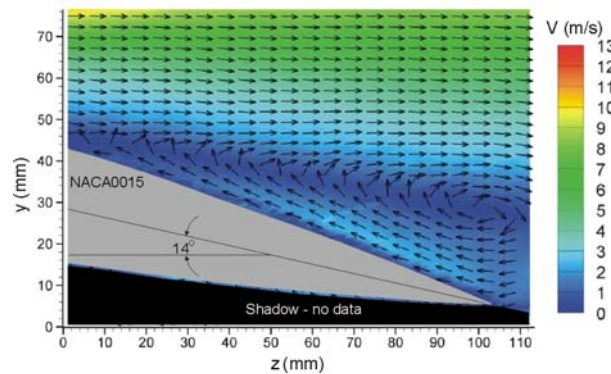


Fig.9. Time-averaged contour velocity map of the airflow around the NACA 0015 airfoil model. Free stream velocity  $V_0 = 10 \text{ m/s}$ ; angle of attack  $14^\circ$ . Plasma OFF – separated airflow

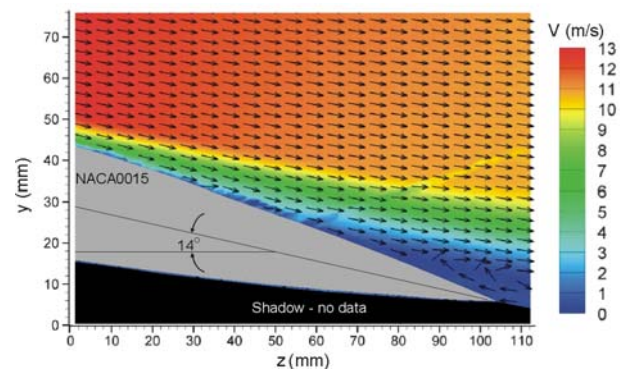


Fig.10. Time-averaged contour velocity map of the airflow around the NACA 0015 airfoil model. Free stream velocity  $V_0 = 10 \text{ m/s}$ ; angle of attack  $14^\circ$ . Plasma ON – airflow reattached. The applied sine-wave voltage was  $15 \text{ kV}_{pp}$  and the frequency was 1.5 kHz

### Summary

The ability of the multi-DBD plasma actuator with floating interelectrode to influence on the flow around the airfoil models was investigated. For that purpose 2D PIV measurements were carried out for NACA 0012 and NACA 0015 airfoil models with plasma actuator fixed on their surface.

The results obtained for leading edge (NACA 0012) and trailing edge (NACA 0015) flow separation control experiments showed that our multi-DBD actuator is capable of postpone the airfoil stall for flows with Reynolds numbers of the order of  $10^5$ . Such a result brings us to a conclusion that our multi-DBD actuator with floating interelectrode can be attractive for some aerodynamic applications.

However, more investigations are needed for the DBD plasma actuators development. The new actuators should effectively influence on the airflow around aerodynamic elements at higher airflow velocities and Reynolds numbers.

### Acknowledgments

The research presented in this paper received funding from the European Community, Seventh Framework Programme FP7/2007-2013 under grant agreement no.: 234201 (PLASMAERO – Useful PLASMas for AERodynamic control [www.plasmaero.eu](http://www.plasmaero.eu)) and by the R. Szewalski Institute of Fluid Flow Machinery, Polish Academy of Sciences, Gdańsk.

## REFERENCES

- [1] Roth J. R., Sherman D. M., and Wilkinson S. P., Boundary layer flow control with a one atmosphere uniform glow discharge surface, *AIAA*, Reno, USA, #98-0328, 1998
- [2] Moreau E., Airflow control by non-thermal plasma actuators, *J. Phys. D: Appl. Phys.* 40, 3, 2007
- [3] Touchard G., Plasma actuators for aeronautics applications - State of art review, *I. J. PEST*, 2, 1, 2008
- [4] Sosa R., Artana G., Moreau E., Touchard G., Stall control at high angle of attack with plasma sheet actuators, *Exp. in Fluids*, 42, 2007
- [5] Jolibois J., Forte M., Moreau E., Application of an AC barrier discharge actuator to control airflow separation above a NACA 0015 airfoil: Optimization of the actuation location along the chord, *J. Electrostatics* 66, 2008
- [6] Corke T., Post M., Orlov D., Single dielectric barrier discharge plasma enhanced aerodynamics: physics, modeling and applications, *Exp. Fluids*, 46, 2009
- [7] Grundmann S., Tropea C., Experimental damping of boundary-layer oscillations using DBD plasma actuators, *Int. J. Heat and Fluid Flow*, 30, 2009
- [8] Little J., Nishihara M., Adamovich I., Samimy M., High-lift airfoil trailing edge separation control using a single dielectric barrier discharge plasma actuator, *Exp Fluids* 48, 2010
- [9] Berendt A., Podlinski J., Mizeraczyk J., Comparison of airflow patterns produced by DBD actuators with smooth or saw-like discharge electrode, *J. Phys. Conf. Series*, 301, 2011

**Authors:** M.Sc. Artur Berendt [aberendt@imp.gda.pl](mailto:aberendt@imp.gda.pl) and Dr. Janusz Podliński [janusz@imp.gda.pl](mailto:janusz@imp.gda.pl), Centre for Plasma and Laser Engineering, The Szewalski Institute of Fluid Flow Machinery, Polish Academy of Sciences, Fiszerza 14, 80-952 Gdańsk; Prof. Jerzy Mizeraczyk [jmiz@imp.gda.pl](mailto:jmiz@imp.gda.pl), Centre for Plasma and Laser Engineering, The Szewalski Institute of Fluid Flow Machinery, Polish Academy of Sciences, Fiszerza 14, 80-952 Gdańsk and Department of Marine Electronics, Gdynia Maritime University, Morska 81-87, 81-225 Gdynia